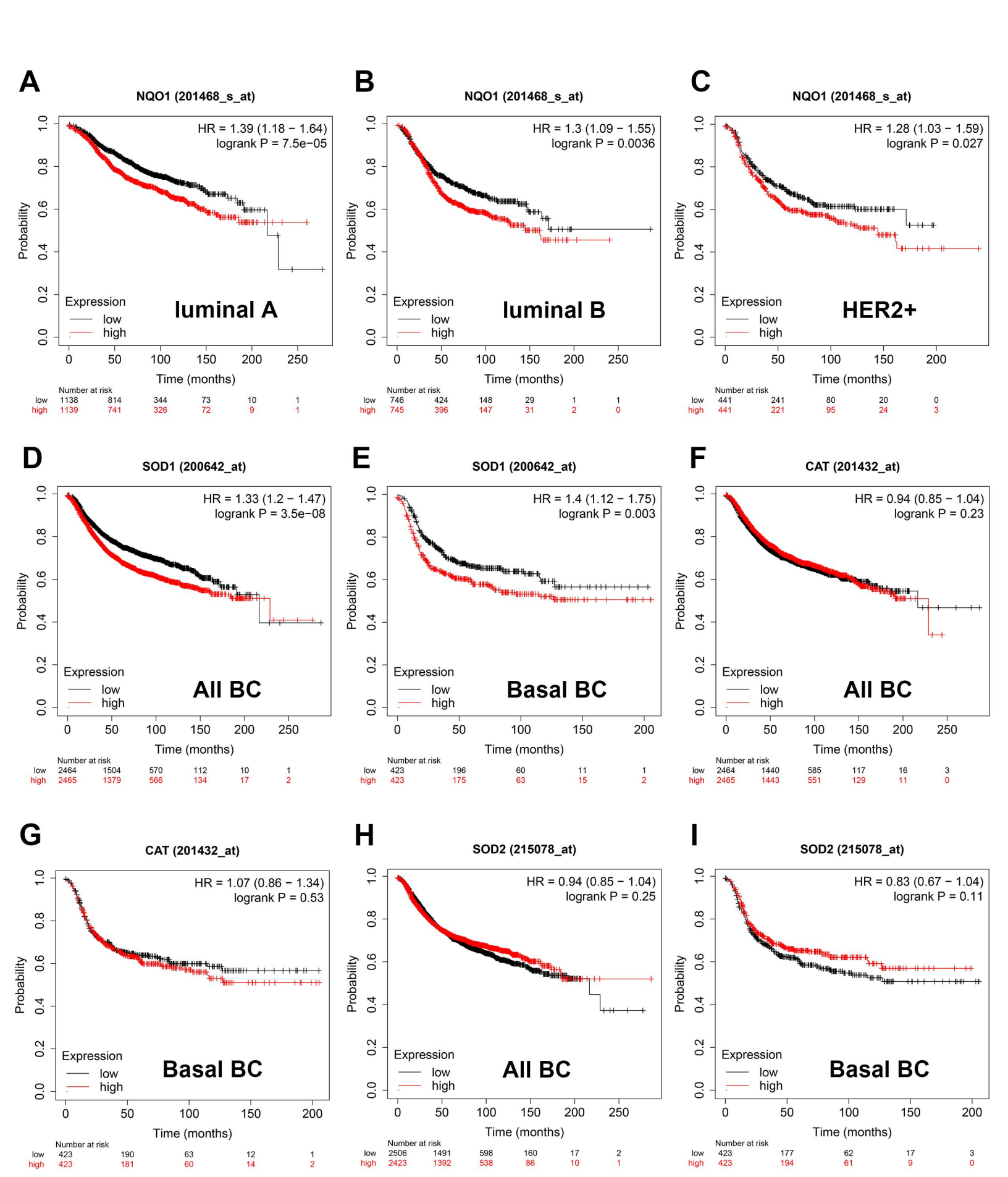
A
NQO1 (201468_s_at)
HR = 1.39 (1.18 − 1.64)
logrank P = 7.5e−05
luminal A
Expression
low
high
Probability
Time (months)
Number at risk
low 1138 814 344 73 10 1
high 1139 741 326 72 9 1
B
NQO1 (201468_s_at)
HR = 1.3 (1.09 − 1.55)
logrank P = 0.0036
luminal B
Number at risk
low 746 424 148 29 1 1
high 745 396 147 31 2 0
C
NQO1 (201468_s_at)
HR = 1.28 (1.03 − 1.59)
logrank P = 0.027
HER2+
Number at risk
low 441 241 80 20 0
high 441 221 95 24 3
D
SOD1 (200642_at)
HR = 1.33 (1.2 − 1.47)
logrank P = 3.5e−08
All BC
Number at risk
low 2464 1504 570 112 10 1
high 2465 1379 566 134 17 2
E
SOD1 (200642_at)
HR = 1.4 (1.12 − 1.75)
logrank P = 0.003
Basal BC
Number at risk
low 423 196 60 11 1
high 423 175 63 15 2
F
CAT (201432_at)
HR = 0.94 (0.85 − 1.04)
logrank P = 0.23
All BC
Number at risk
low 2464 1440 585 117 16 3
high 2465 1443 551 129 11 0
G
CAT (201432_at)
HR = 1.07 (0.86 − 1.34)
logrank P = 0.53
Basal BC
Number at risk
low 423 190 63 12 1
high 423 181 60 14 2
H
SOD2 (215078_at)
HR = 0.94 (0.85 − 1.04)
logrank P = 0.25
All BC
Number at risk
low 2506 1491 598 160 17 2
high 2423 1392 538 86 10 1
I
SOD2 (215078_at)
HR = 0.83 (0.67 − 1.04)
logrank P = 0.11
Basal BC
Number at risk
low 423 177 62 17 3
high 423 194 61 9 0

**Figure S1**. **The expression of NQO1 and SOD1 but not CAT and SOD2 corelates with poor patient survival of BC, related to Figure 1**.

(**A-C**) High NQO1 expression corelates with low recurrence-free survival (RFS) of luminal A (**A**), luminal B (**B**) and HER2+(**C**) BC.

(**D-E**) High SOD1 expression corelates with low RFS of all BC subtypes (**D**) as well as basal BC (**E**).

(**F-G**) CAT expression does not corelate with low RFS of all BC subtypes (**F**) as well as basal BC (**G**).

(**H-I**) SOD2 expression has no corelation with low RFS of all BC subtypes (**H**) as well as basal BC (**I**).

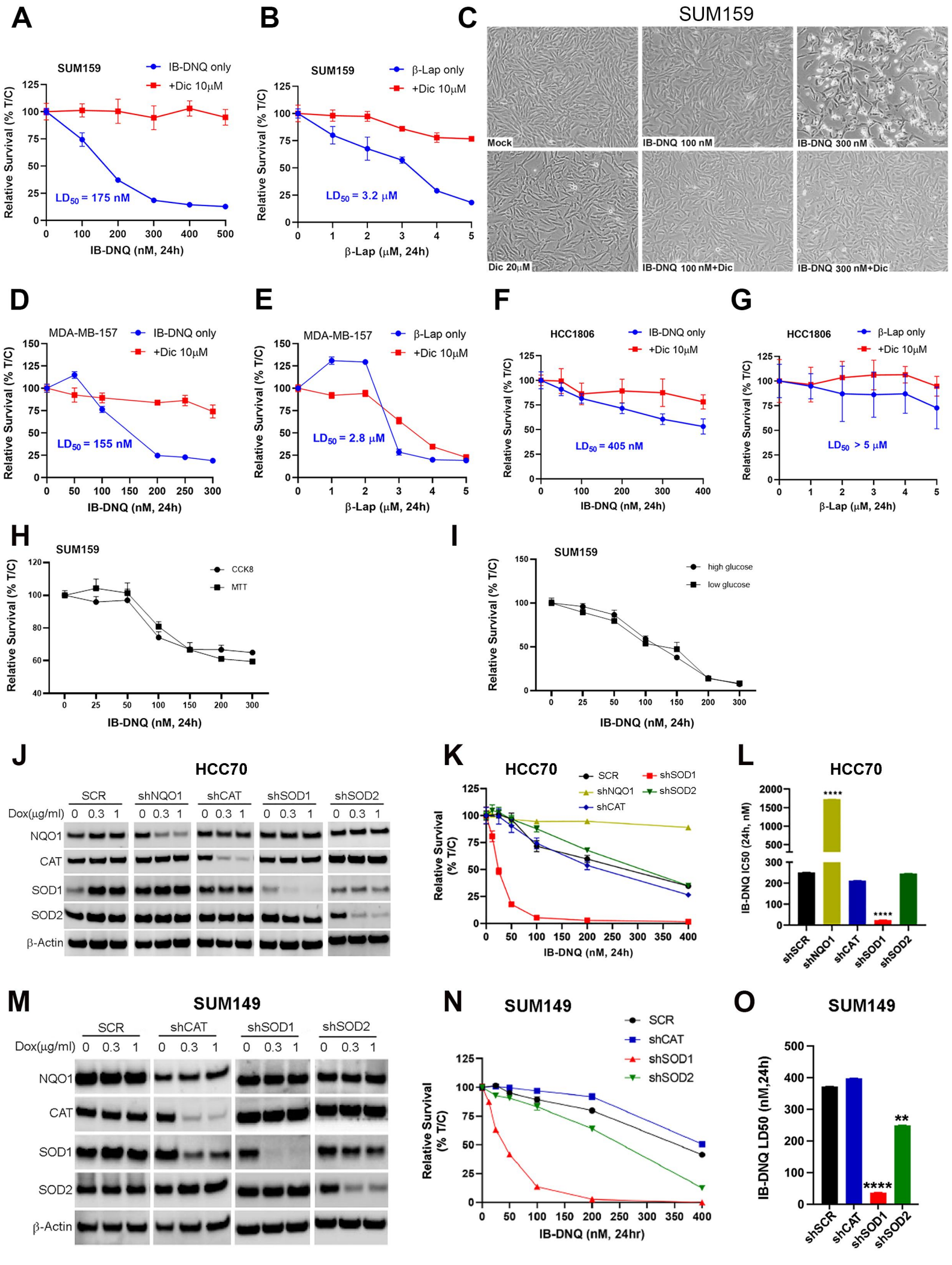
A
SUM159
IB-DNQ only
+Dic 10μM
Relative Survival (% T/C)
LD50 = 175 nM
IB-DNQ (nM, 24h)
B
SUM159
β-Lap only
+Dic 10μM
LD50 = 3.2 μM
β-Lap (μM, 24h)
C
SUM159
Mock
IB-DNQ 100 nM
IB-DNQ 300 nM
Dic 20μM
IB-DNQ 100 nM+Dic
IB-DNQ 300 nM+Dic
D
MDA-MB-157
IB-DNQ only
+Dic 10μM
LD50 = 155 nM
IB-DNQ (nM, 24h)
E
MDA-MB-157
β-Lap only
+Dic 10μM
LD50 = 2.8 μM
β-Lap (μM, 24h)
F
HCC1806
IB-DNQ only
+Dic 10μM
LD50 = 405 nM
IB-DNQ (nM, 24h)
G
HCC1806
β-Lap only
+Dic 10μM
LD50 > 5 μM
β-Lap (μM, 24h)
H
SUM159
CCK8
MTT
IB-DNQ (nM, 24h)
I
SUM159
high glucose
low glucose
IB-DNQ (nM, 24h)
J
HCC70
SCR
shNQO1
shCAT
shSOD1
shSOD2
Dox(μg/ml) 0 0.3 1
NQO1
CAT
SOD1
SOD2
β-Actin
K
HCC70
SCR
shSOD1
shNQO1
shSOD2
shCAT
Relative Survival (% T/C)
IB-DNQ (nM, 24h)
L
HCC70
IB-DNQ IC50 (24h, nM)
shSCR
shNQO1
shCAT
shSOD1
shSOD2
M
SUM149
SCR
shCAT
shSOD1
shSOD2
Dox(μg/ml) 0 0.3 1
NQO1
CAT
SOD1
SOD2
β-Actin
N
SUM149
SCR
shCAT
shSOD1
shSOD2
Relative Survival (% T/C)
IB-DNQ (nM, 24hr)
O
SUM149
IB-DNQ LD50 (nM,24h)
shSCR
shCAT
shSOD1
shSOD2

**Figure S2**. **IB-DNQ is more potent and specific than β-lap in killing TNBC cells and Dox-induced KD of SOD1 specifically enhances IB-DNQ's efficacy in killingTNBC cells, related to Figure 2**.

(**A-B**) Comparison of $LD_{50}$ of IB-DNQ (A) vs. β-lap (B) in SUM159 BC cells treated with each compound alone or together with the NQO1 inhibitor DIC. Error bars denote SEM (n=6).

(**C**) SUM159 BC cells treated with Mock (DMSO), DIC (20 μM), IB-DNQ (100 or 300nM) alone, or combination of IB-DNQ (100 or 300nM) and DIC (20μM) for 24h and examined by light microscopy.

(**D-E**) Comparison of $LD_{50}$ of IB-DNQ (D) vs. β-lap (E) in MDA-MB-157 BC cells treated with each compound alone or together with NQO1 inhibitor DIC. Error bars denote SEM (n=6).

(**F-G**) Comparison of $LD_{50}$ of IB-DNQ (F) vs. β-lap (G) in $NQO1^{lo}$ HCC1806 BC cells treated with each compound alone or together with NQO1 inhibitor DIC. Error bars denote SEM (n=6).

(**H**) Relative survival of SUM159 BC cells treated with different doses of IB-DNQ measured by MTT vs. CCK8 assay. Error bars denote SEM (n=6).

(**I**) Relative survival of SUM159 BC cells treated with different doses of IB-DNQ in media containing high (25 mM) or low (5.5 mM) of glucose by CCK8 assay. Error bars denote SEM (n=6)

(**J-L**) Dox-inducible KD of NQO1, CAT, SOD1 and SOD2 in HCC70 BC cells validated by immunoblotting with respective antibodies (**J**), and KD of NQO1 renders HCC70 BC cells resistant to IB-DNQ treatment, while KD of SOD1, but not CAT or SOD2, in HCC70 significantly enhanced IB-DNQ-elicited lethality (**K** and **L**). ****: $p < 0.0001$ vs. shSCR (n=2, one-way ANOVA). Error bars denote SEM.

(**M-O**) Dox-inducible KD of CAT, SOD1 and SOD2 in $NQO1^{lo}$ SUM149 BC cells validated by immunoblotting with respective antibodies (**M**), and KD of SOD1 or SOD2 but not CAT in SUM149 significantly enhanced IB-DNQ-elicited lethality (**M** and **O**). **, ****: $p < 0.01$ and 0.0001 vs. shSCR (n=2, one-way ANOVA). Error bars denote SEM.

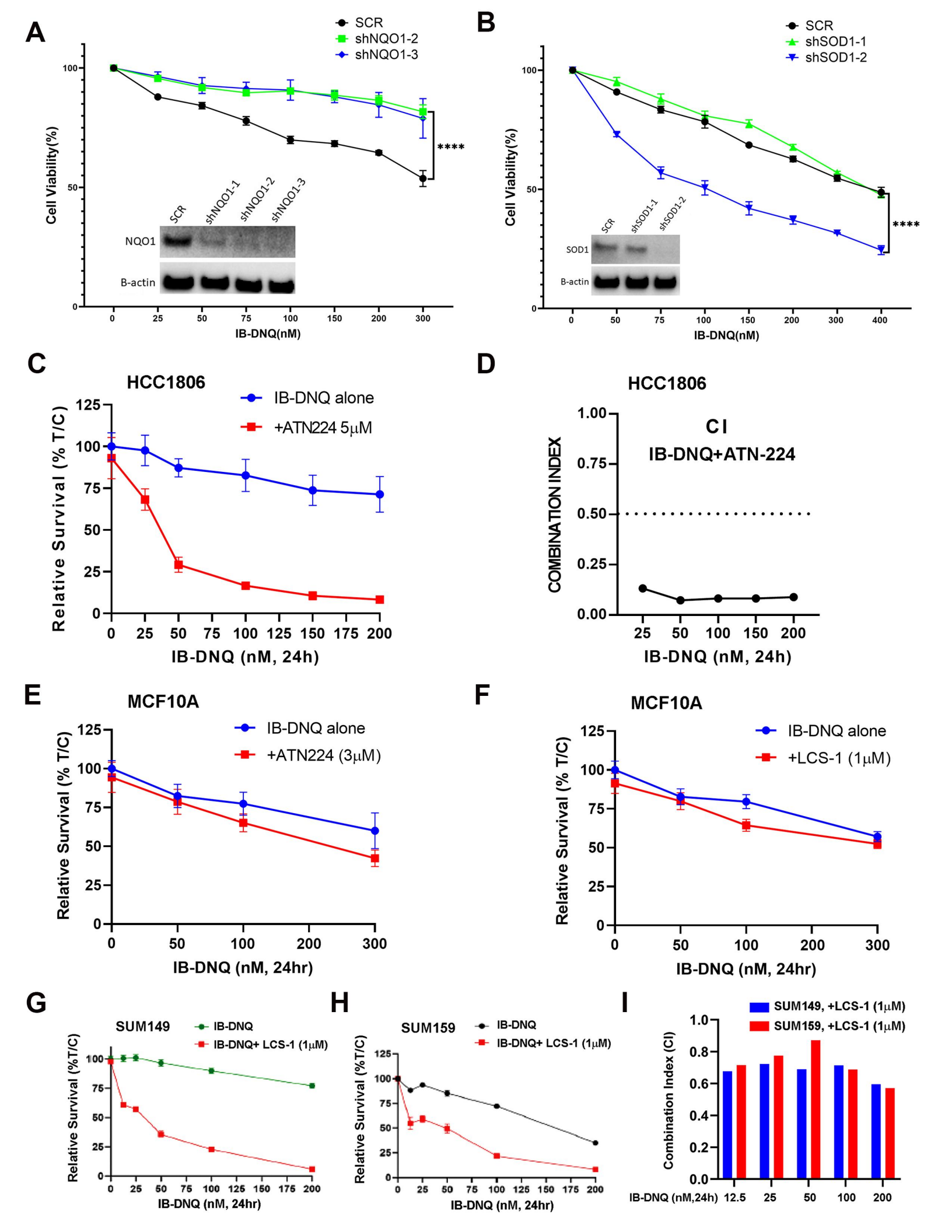
A
SCR
shNQO1-2
shNQO1-3
Cell Viability(%)
IB-DNQ(nM)
****
SCR
shNQO1-1
shNQO1-2
shNQO1-3
NQO1
B-actin
B
SCR
shSOD1-1
shSOD1-2
Cell Viability(%)
IB-DNQ(nM)
****
SCR
shSOD1-1
shSOD1-2
SOD1
B-actin
C
HCC1806
IB-DNQ alone
+ATN224 5μM
Relative Survival (% T/C)
IB-DNQ (nM, 24h)
D
HCC1806
CI
IB-DNQ+ATN-224
COMBINATION INDEX
IB-DNQ (nM, 24h)
E
MCF10A
IB-DNQ alone
+ATN224 (3μM)
Relative Survival (% T/C)
IB-DNQ (nM, 24hr)
F
MCF10A
IB-DNQ alone
+LCS-1 (1μM)
Relative Survival (% T/C)
IB-DNQ (nM, 24hr)
G
SUM149
IB-DNQ
IB-DNQ+ LCS-1 (1μM)
Relative Survival (%T/C)
IB-DNQ (nM, 24hr)
H
SUM159
IB-DNQ
IB-DNQ+ LCS-1 (1μM)
Relative Survival (%T/C)
IB-DNQ (nM, 24hr)
I
SUM149, +LCS-1 (1μM)
SUM159, +LCS-1 (1μM)
Combination Index (CI)
IB-DNQ (nM,24h) 12.5 25 50 100 200

**Figure S3**. **SOD1 inhibitor ATN224 synergistically enhances IB-DNQ's efficacy in killingTNBC but not nontumorigenic mammary epithelial cell MCF10A, related to Figure 2**.

(**A**) Dox-induced KD of NQO1 in SUM159 BC cells with three different SMARTvector Dox-inducible lentiviral shRNA clones to validate the effect of knockdown of NQO1 expression in affecting IB-DNQ sensitivity, which is measured by MTT assay. ****: p< 0.0001 (shNQO1-2 or shNQO1-3 vs. shSCR, n=6, two-way ANOVA). Error bars denote SEM.

(**B**) Dox-induced KD of SOD1 in SUM159 BC cells with two SMARTvector Dox-inducible lentiviral shRNA clones to validate the effect of knockdown of SOD1 expression in affecting IB-DNQ sensitivity, measured by MTT assay. ****: p< 0.0001 (shSOD1-2 vs. shSCR or shSOD1-1, n=6, two-way ANOVA). Error bars denote SEM.

(**C-D**) Relative survival of $NQO1^{lo}$ HCC1806 BC cells treated with IB-DNQ alone or together with SOD1 inhibitor ATN224 (**C**, n=6) and combination index (CI) of ATN224 (at 5 μM) with sublethal doses of IB-DNQ ranging from 12.5-200 nM in HCC1806 (**D**). Error bars denote SEM.

(**E-F**) Relative survival of $NQO1^{lo}$ MCF10A cells treated with with IB-DNQ alone or together with SOD1 inhibitor ATN224 (**E,** n=6) or LCS-1 (**F,** n=6). Error bars denote SEM.

(**G-I**) Relative survival of SUM149 (**G,** n=6**)** and SUM159 (**H,** n=6) TNBC cells treated with IB-DNQ alone or together with SOD1 inhibitor LCS-1, and combination index (CI) of LCS-1 (at 1 μM) together with variousl doses of IB-DNQ ranging from 12.5-200 nM in SUM149 and SUM159 BC cells (**I**). Error bars denote SEM.

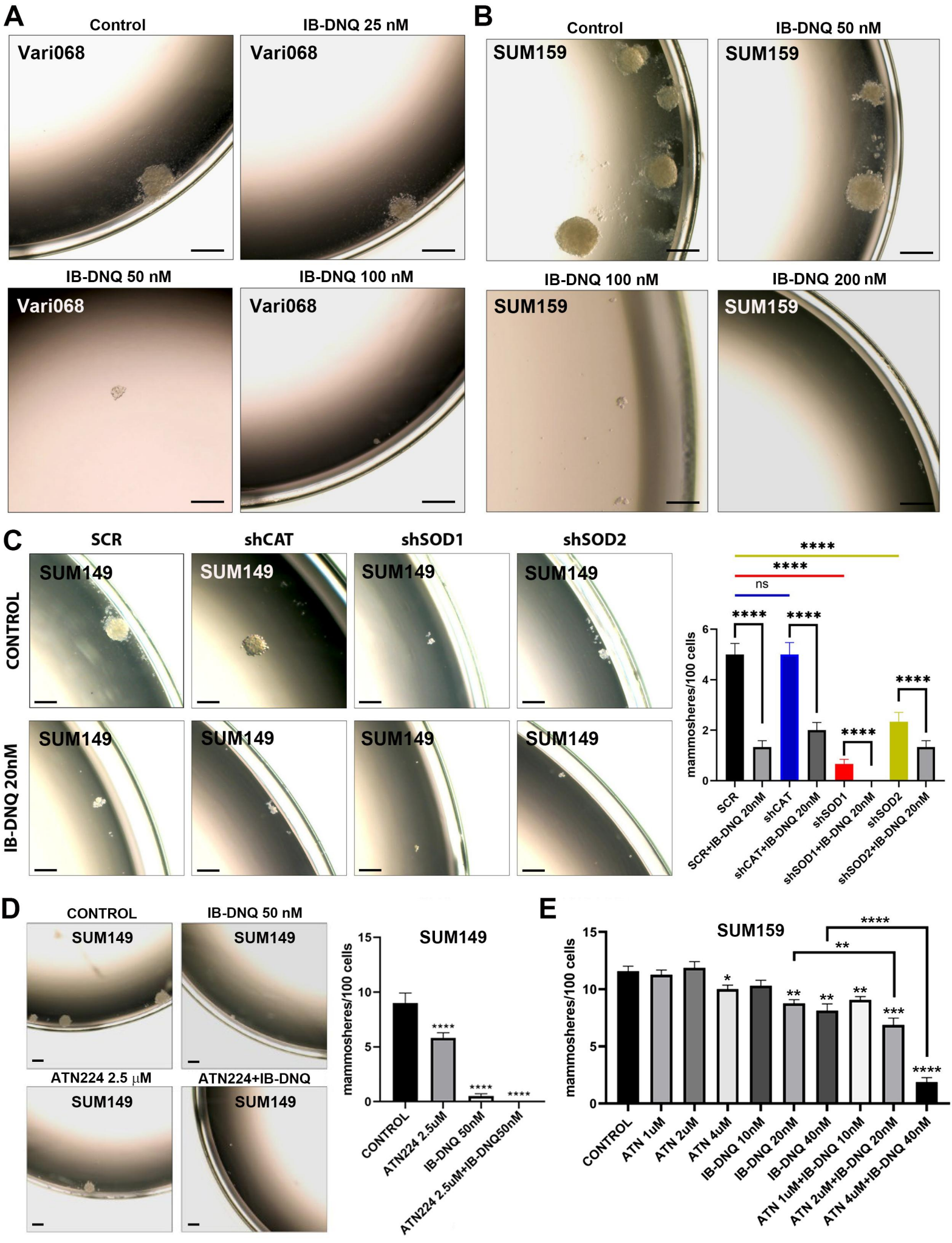
A
Control
IB-DNQ 25 nM
Vari068
Vari068
IB-DNQ 50 nM
IB-DNQ 100 nM
Vari068
Vari068
B
Control
IB-DNQ 50 nM
SUM159
SUM159
IB-DNQ 100 nM
IB-DNQ 200 nM
SUM159
SUM159
C
SCR
shCAT
shSOD1
shSOD2
CONTROL
IB-DNQ 20nM
SUM149
mammosheres/100 cells
****
ns
SCR
SCR+IB-DNQ 20nM
shCAT
shCAT+IB-DNQ 20nM
shSOD1
shSOD1+IB-DNQ 20nM
shSOD2
shSOD2+IB-DNQ 20nM
D
CONTROL
IB-DNQ 50 nM
ATN224 2.5 μM
ATN224+IB-DNQ
SUM149
SUM149
SUM149
SUM149
SUM149
mammosheres/100 cells
CONTROL
ATN224 2.5uM
IB-DNQ 50nM
ATN224 2.5uM+IB-DNQ50nM
E
SUM159
mammosheres/100 cells
CONTROL
ATN 1uM
ATN 2uM
ATN 4uM
IB-DNQ 10nM
IB-DNQ 20nM
IB-DNQ 40nM
ATN 1uM+IB-DNQ 10nM
ATN 2uM+IB-DNQ 20nM
ATN 4uM+IB-DNQ 40nM

**Figure S4**. **IB-DNQ preferentially inhibits CSC activity and genetic or phamacological inhibition of SOD1 potentiate the efficacy of IB-DNQ in supressing tumorsphere-forming capacity of TNBC cells, related to Figure 3**.

(**A-B**) Tumorsphere formation of Vari068 (**A**) and SUM159 (**B**) BC cells sorted into 96-well ultralow-attachment plates at density of 20 cells/well. Bar: 200 μm.

(**C**) Tumorsphere formation assay at clonal density (20 cells/well) was performed to examine the effects of Dox (0.5 μg/ml) induced KD of CAT, SOD1 or SOD2 vs. SCR in affecting sphere-forming capacity of SUM149 BC cells and their impact on IB-DNQ-mediated suppression of tumorsphere formation. Bar: 200 μm. ****: $P < 0.0001$ (n=3, one-way ANOVA). Error bars denote SEM.

(**D**) Tumorsphere formation of SUM149 BC cells treated with vehicle (DMSO), IB-DNQ (50nM), ATN224 (2.5 μM), or IB-DNQ (50nM) plus ATN224 (2.5 μM). Bar: 200 μm. ****: $P < 0.0001$ (n=3, one-way ANOVA). Error bars denote SEM.

(**E**) Tumorsphere formation of SUM159 BC cells treated with vehicle (DMSO), ATN224 (1-4 μM), IB-DNQ (10-40 nM) or IB-DNQ plus ATN224 at different doses. *, **, ***, ****: $P < 0.05$, 0.01, 0.001 or 0.0001 (vs. Control, n=3, one-way ANOVA). Error bars denote SEM.

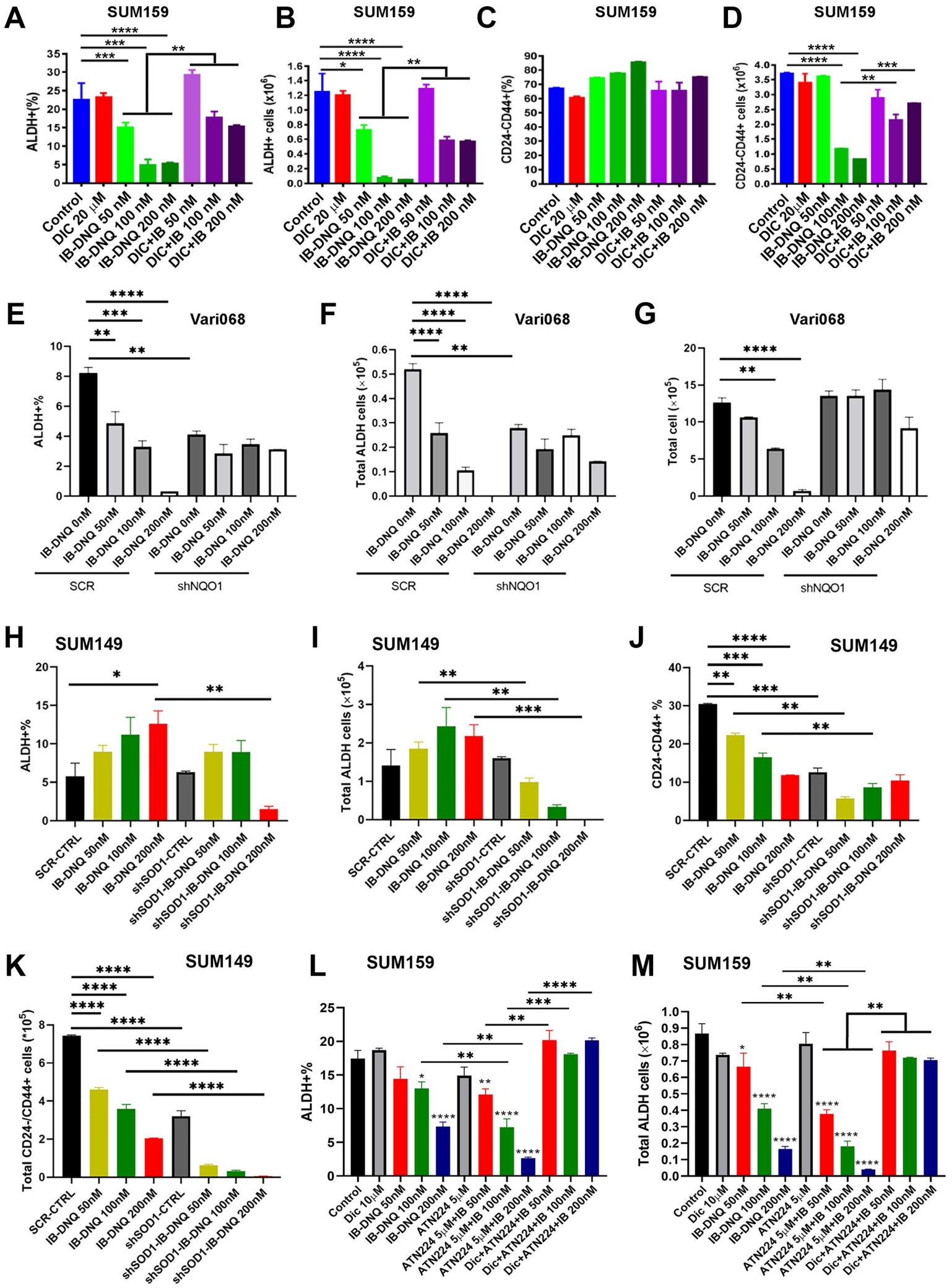
A
SUM159
ALDH+(%)
Control
DIC 20 μM
IB-DNQ 50 nM
IB-DNQ 100 nM
IB-DNQ 200 nM
DIC+IB 50 nM
DIC+IB 100 nM
DIC+IB 200 nM
B
SUM159
ALDH+ cells (x10^6)
C
SUM159
CD24-CD44+(%)
D
SUM159
CD24-CD44+ cells (x10^6)
E
Vari068
ALDH+%
IB-DNQ 0nM
IB-DNQ 50nM
IB-DNQ 100nM
IB-DNQ 200nM
SCR
shNQO1
F
Vari068
Total ALDH cells (×10^5)
G
Vari068
Total cell (×10^5)
H
SUM149
ALDH+%
SCR-CTRL
IB-DNQ 50nM
IB-DNQ 100nM
IB-DNQ 200nM
shSOD1-CTRL
shSOD1-IB-DNQ 50nM
shSOD1-IB-DNQ 100nM
shSOD1-IB-DNQ 200nM
I
SUM149
Total ALDH cells (×10^5)
J
SUM149
CD24-CD44+ %
K
SUM149
Total CD24-/CD44+ cells (*10^5)
L
SUM159
ALDH+%
Control
Dic 10μM
IB-DNQ 50nM
IB-DNQ 100nM
IB-DNQ 200nM
ATN224 5μM
ATN224 5μM+IB 50nM
ATN224 5μM+IB 100nM
ATN224 5μM+IB 200nM
Dic+ATN224+IB 50nM
Dic+ATN224+IB 100nM
Dic+ATN224+IB 200nM
M
SUM159
Total ALDH cells (×10^6)

**Figure S5**. **IB-DNQ preferentially inhibits ALDH+ CSCs in a NQO1-dependent manner and genetic or phamacological inhibition of SOD1 potentiate the efficacy of IB-DNQ in supressing both ALDH+ E- and CD24-CD44+ M-CSC-like cells, related to Figure 3**.

(**A-D**) SUM159 BC cells were treated with Control (DMSO), DIC (20 μM), IB-DNQ (50-200 nM) alone or IB-DNQ together DIC for 20h, and examined by flow cytometry to measure the content and absolute number of ALDH+ (**A** and **B**) and CD24-CD44+ (**C** and **D**) CSC-like cells. *, **, ***,****: P< 0.05, 0.01, 0.001 or 0.0001 respectively (n=3). Error bars denote SEM.

(**E-G**) Vari068 BC cells expressing SCR or shNQO1 were pretreated with Dox (0.5 μg/ml) for 48h and then treated with different doses of IB-DNQ (0-200nM) for 20h to examine the percentage and total number of ALDH+ CSCs. **, ***,****: P< 0.01, 0.001，0.0001 respectively (n=3). Error bars denote SEM.

(**H-K**) SUM149 BC cells expressing SCR or shSOD1 were pretreated with Dox (0.5 μg/ml) for 48h, and then treated with different doses of IB-DNQ (50, 100, 200nM) for 20h to examine the percentage and total number of ALDH+ and CD24-CD44+ CSCs. *, **, ***,****: P< 0.05, 0.01, 0.001，0.0001 respectively (n=3). Error bars denote SEM.

(**L-M**) SUM159 BC cells were treated with Control (DMSO), DIC (10 μM), IB-DNQ (50-200 nM), ATN224 (5 μM) alone or IB-DNQ together with ATN224 and/or DIC for 20h, and examined by flow cytometry to measure the content (L) and absolute number (M) of ALDH+ CSCs. *, **, ***,****: P< 0.05, 0.01, 0.001 or 0.0001 respectively vs. Control or indicated with brackets (n=3). Error bars denote SEM.

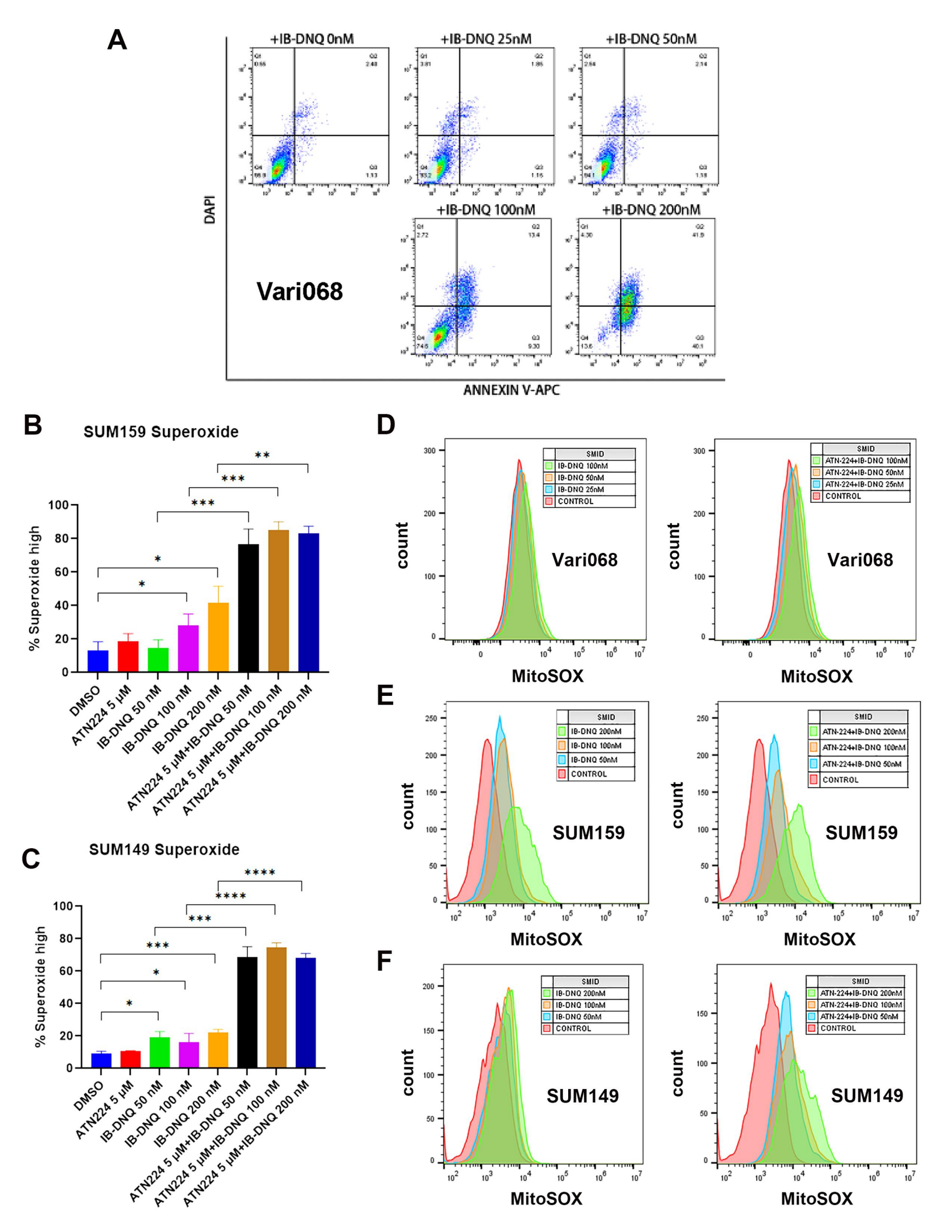
A
+IB-DNQ 0nM
+IB-DNQ 25nM
+IB-DNQ 50nM
+IB-DNQ 100nM
+IB-DNQ 200nM
DAPI
Vari068
ANNEXIN V-APC
B
SUM159 Superoxide
% Superoxide high
DMSO
ATN224 5 μM
IB-DNQ 50 nM
IB-DNQ 100 nM
IB-DNQ 200 nM
ATN224 5 μM+IB-DNQ 50 nM
ATN224 5 μM+IB-DNQ 100 nM
ATN224 5 μM+IB-DNQ 200 nM
C
SUM149 Superoxide
% Superoxide high
D
SMID
IB-DNQ 100nM
IB-DNQ 50nM
IB-DNQ 25nM
CONTROL
ATN-224+IB-DNQ 100nM
ATN-224+IB-DNQ 50nM
ATN-224+IB-DNQ 25nM
Vari068
count
MitoSOX
E
IB-DNQ 200nM
ATN-224+IB-DNQ 200nM
SUM159
F
SUM149

**Figure S6**. **IB-DNQ treatment induces apoptotic death of TNBC cells overexpressing NQO1 and SOD1 inhibitor ATN224 potentiates the ability of IB-DNQ to elevate mitoROS in TNBC expressing different levels of NQO1, related to Figure 4 and Figure 5**.

(**A**) IB-DNQ treatment dose-dependently induces apoptosis of $NQO^{hi}$ Vari068 BC cells as examined by Annexin V labeling and flow cytometry, related to Figure 4.

(**B-C**) Measurement of cellular superoxide levels in SUM159 (**B**) and SUM149 (**C)** BC cells treated with vehicle (DMSO) and different doses of IB-DNQ alone or together with ATN224. *, **, ***, ****: $P < 0.05$, 0.01, 0.001 and 0.0001 vs. Control or indicated with brackets (n=3). Error bars denote SEM.

(**D-F**) Vari068 (**D**), SUM159 (**E**) and SUM149 (**F**) BC cells treated with different doses of IB-DNQ alone or IB-DNQ plus ATN224 were stained with MitoSOX red (2.5 μM) and mean fluorescence intensity (MFI) of MitoSOX red was analyzed in each condition by flow cytometry, related to Figure 5.

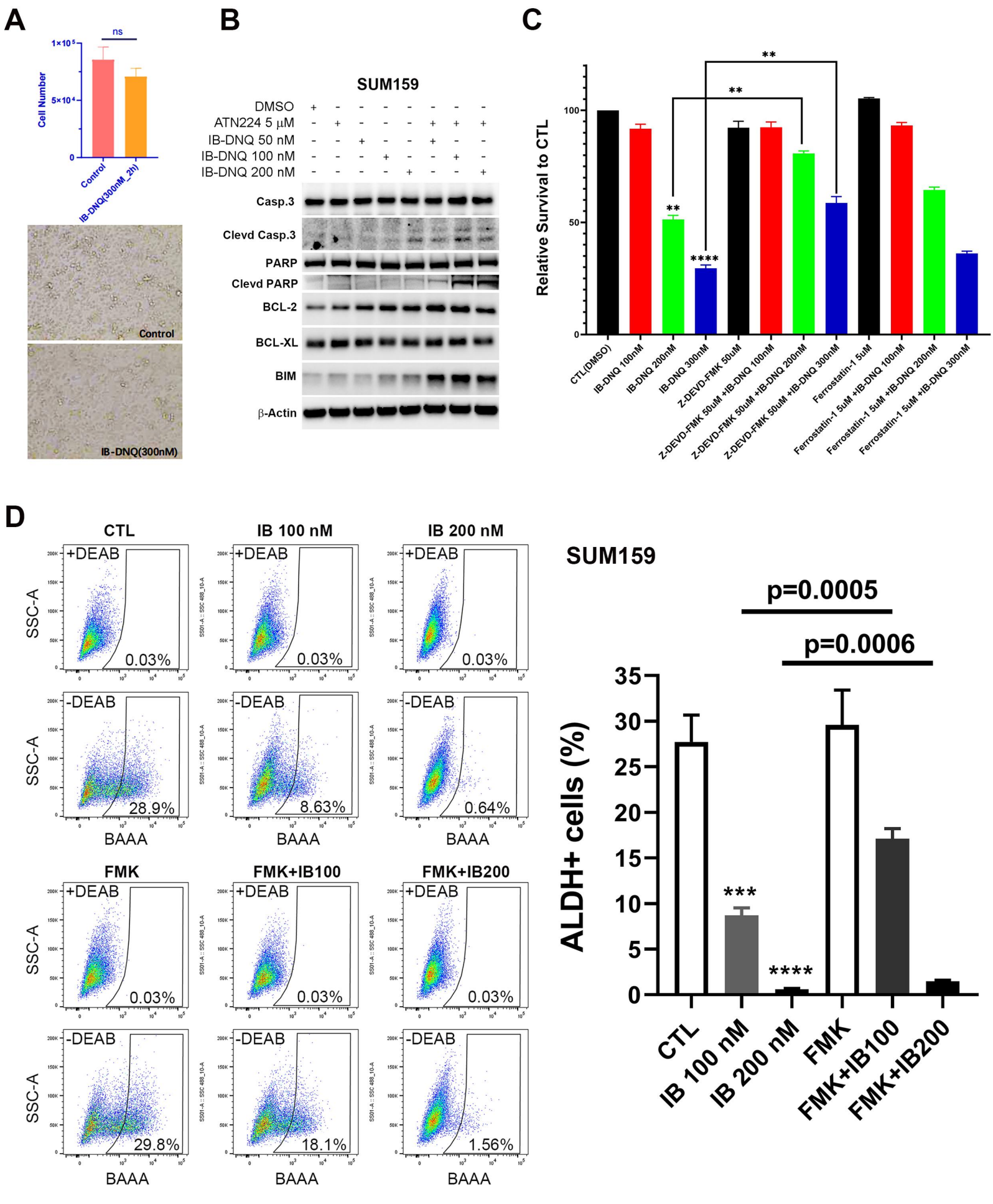
A
ns
Cell Number
1×10⁵
5×10⁴
0
Control
IB-DNQ(300nM_2h)
Control
IB-DNQ(300nM)
B
SUM159
DMSO
ATN224 5 μM
IB-DNQ 50 nM
IB-DNQ 100 nM
IB-DNQ 200 nM
Casp.3
Clevd Casp.3
PARP
Clevd PARP
BCL-2
BCL-XL
BIM
β-Actin
C
Relative Survival to CTL
100
50
0
**
**
**
****
CTL(DMSO)
IB-DNQ 100nM
IB-DNQ 200nM
IB-DNQ 300nM
Z-DEVD-FMK 50uM
Z-DEVD-FMK 50uM +IB-DNQ 100nM
Z-DEVD-FMK 50uM +IB-DNQ 200nM
Z-DEVD-FMK 50uM +IB-DNQ 300nM
Ferrostatin-1 5uM
Ferrostatin-1 5uM +IB-DNQ 100nM
Ferrostatin-1 5uM +IB-DNQ 200nM
Ferrostatin-1 5uM +IB-DNQ 300nM
D
CTL
IB 100 nM
IB 200 nM
FMK
FMK+IB100
FMK+IB200
+DEAB
-DEAB
SSC-A
BAAA
0.03%
28.9%
8.63%
0.64%
0.03%
0.03%
0.03%
0.03%
29.8%
18.1%
1.56%
SUM159
p=0.0005
p=0.0006
ALDH+ cells (%)
35
30
25
20
15
10
5
0
***
****
CTL
IB 100 nM
IB 200 nM
FMK
FMK+IB100
FMK+IB200

**Figure S7**. **IB-DNQ induced cell death and abrogation of ALDH+ BCSCs in SUM159 is rescued by Casp 3 inhibitor Z-DEVD-FMK, related to Figure 6**.

(**A**) SUM159 BC cells treated with 300 nM of IB-DNQ for 2h were examined by CCK8 assay (upper panel) and optical microscopy (lower panels) to examine the viability of SUM159 BC cells (n=3). ns: not significantly different.

(**B**) SUM159 BC cells were treated with vehicle, ATN224 (5 μM), and 50-200 nM of IB-DNQ alone or in combination with ATN224 for 20h, and subjected to immunoblotting to examine the activation of Casp3 and the cleavage of its substrate PARP, as well as the expression of anti- and pro-apoptotic BCL2 family proteins.

(**C**) SUM159 BC cells treated with CTL(DMSO), Z-DEVD-FMK (50 μM), Ferrostatin-1 (5 μM) or IB-DNQ (100-300nM) alone, or combination of IB-DNQ with Z-DEVD-FMK or Ferrostatin-1 for 4h, and relative suvival of SUM159 BC were measured with MTT assay (n=6). **, ****: P< 0.01 or 0.0001 (vs. CTL or indicated with brackets). Data are representatives of two independent experiments.

(**D**) SUM159 BC cells treated with Mock (DMSO), Z-DEVD-FMK (50 μM), IB-DNQ (100-200nM) alone, or combination of IB-DNQ and Z-DEVD-FMK for 3h and examined for ALDH+ CSCs by Aldefluor assay and flow cytometry (left panel). The proprotion of ALDH+ CSCs in each condition was plotted based on 3 independent experiments (right panel). ***, ****: P< 0.001 and 0.0001 respectively vs. CTL (DMSO). Error bars denote SD (stardard deviations). DEAB: the inhibitor of ALDH enzymatic activity. BAAA: the substrate of ALDH enzymatic activity.

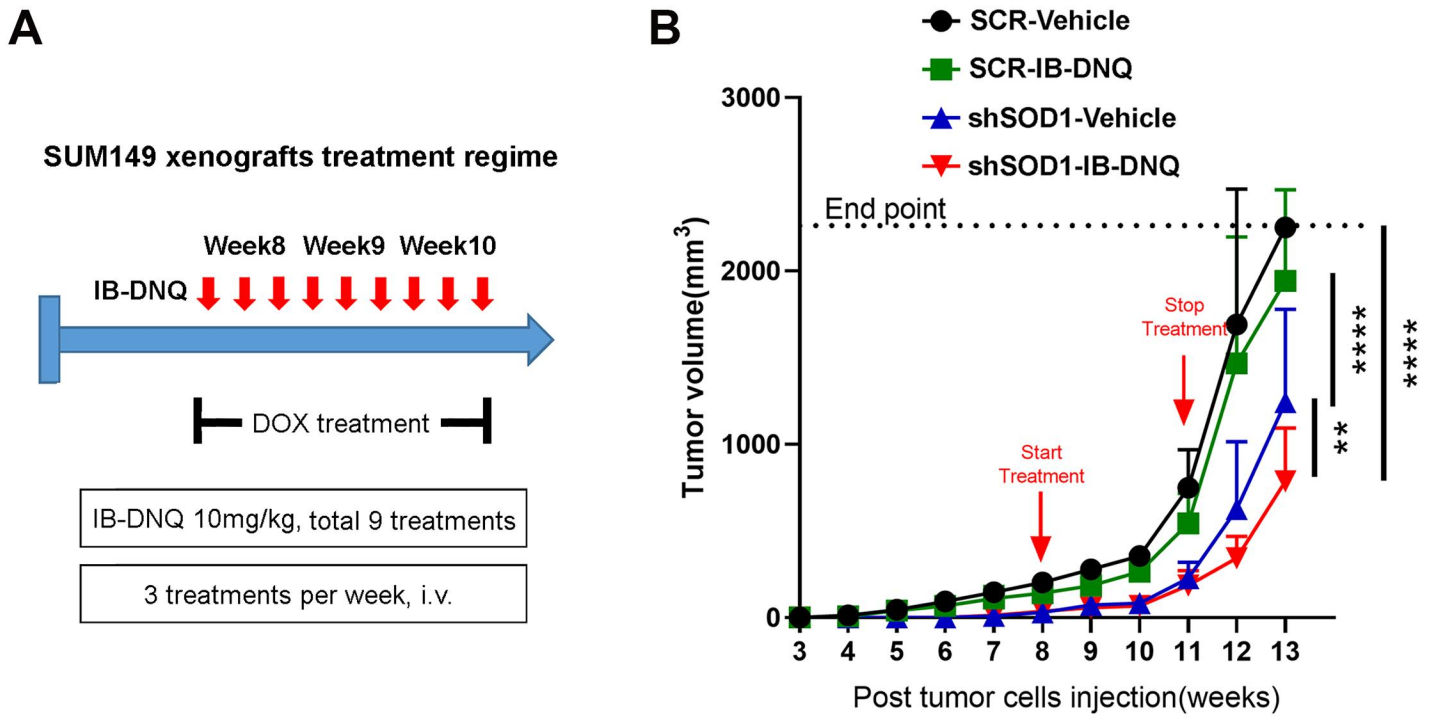


**Figure S8. Dox-inducied KD of SOD1 suppresses tumor growth of SUM149 BC cells and IB-DNQ treatment further enhances tumor growth retardation of SOD1 KD cells, related to Figure 7.**

(**A**) SUM149 BC cells expressing Dox-inducible KD (shSOD1) or scrambled control (SCR) were injected into the #4 MFP of 7-wk-old female SCID mice, and mice bearing mammary tumors (3-4 mm in diameter) expressing shSOD1 or SCR sequence were each randomized into two groups (6 mice/group) and subject to treatment with Dox (200 μg/ml in water) plus vehicle (20% HPβCD, I.V.) or IB-DNQ (10 mg/kg, I.V.) for 3 weeks.

(**B**) Tumor growth of SUM149 BC cells expressing SCR or shSOD1 after treated with Dox (200 μg/ml in water) plus vehicle or IB-DNQ. **, ****: P< 0.01 or 0.0001 respectively (n=6, two-way ANOVA). Error bars denote SD.

## KEY RESOURCES TABLE

| REAGENT or RESOURCE | SOURCE | IDENTIFIER |
|---|---|---|
| Antibodies and Labeling Reagents | | |
| Anti-ALDH1A1 | Invitrogen | Cat# MA5-29023 RRID: AB_2784960 |
| Anti-ALDH1A3 | Invitrogen | Cat# PA5-29188 RRID: AB_2546664 |
| Anti-BCL-2 | Cell Signaling Technology | Cat# 15071S |
| Anti-BCL-xL | Cell Signaling Technology | Cat# 2764S |
| Anti-β-Actin | Cell Signaling Technology | Cat# 4970S |
| Anti-Bim | Cell Signaling Technology | Cat# 2933S |
| Anti-Caspase-3 | Cell Signaling Technology | Cat# 9662S |
| Anti-Cleaved Caspase-3 | Cell Signaling Technology | Cat# 9661S |
| Anti-Catalase | Cell Signaling Technology | Cat# 12980S |
| Anti-Cytochrome c | Cell Signaling Technology | Cat# 12963S |
| Anti-Ki67 | Cell Signaling Technology | Cat# 12202S |
| Anti-NQO1 | Cell Signaling Technology | Cat# 62262S |
| Anti NRF2 | Cell Signaling Technology | Cat# 12721S |
| Anti-p-H2A.X | Cell Signaling Technology | Cat# 2577S |
| Anti-PARP | Cell Signaling Technology | Cat# 9542S |
| Anti-Cleaved PARP | Cell Signaling Technology | Cat# 5625S |
| Anti-SDHA | Cell Signaling Technology | Cat# 5839S |
| Anti-Skp1 | Cell Signaling Technology | Cat# 2156S |

| | | |
|---|---|---|
| Anti-SOD1 | Cell Signaling Technology | Cat# 37385S |
| Anti-SOD1 | Cell Signaling Technology | Cat# 4266S |
| Anti-SOD2 | Cell Signaling Technology | Cat# 13141S |
| Anti-VDAC | Cell Signaling Technology | Cat# 4661S |
| Anti-Rabbit IgG, HRP Linked Antibody | Cell Signaling Technology | Cat# 7074S |
| Anti-Mouse IgG, HRP Linked Antibody | Cell Signaling Technology | Cat# 7076S |
| APC mouse Anti-human CD44 | BD Biosciences | Cat# 559942 RRID: AB_398683 |
| APC anti-mouse H-2K[d] | BioLegend | Cat# 116620 AB_10645328 |
| FITC Anti-human CD24 | BD Biosciences | Cat# 560992 RRID: AB_10562033 |
| FITC Anti-human CD44 | BD Biosciences | Cat# 555478 RRID:AB_39587 0 |
| PE anti-mouse H-2K[d] | BD Biosciences | Cat# 553566 RRID: AB_394924 |
| PE/Cy7 Anti-human CD24 | BD Biosciences | Cat# 561646 AB_10892826 |
| PE/Cy7 Anti-human CD24 | BioLegend | Cat# 311120 AB_2259843 |
| DAPI | Sigma-Aldrich | Cat# D9542 |
| APC Annexin V | BD Biosciences | Cat#550474 AB_2868885 |
| CellROX® Orange Reagent | Thermo Fisher Scientific | Cat# C10443 |
| MitoSOX™ Red | Thermo Fisher Scientific | Cat# M36008 |
| Chemicals, Peptides, and Recombinant Proteins | | |
| ATN224 | Cayman Chemical | Cat# 23553 CAS: 649749-10-0 |
| 3-AT | Sigma-Aldrich | Cat# A8056 CAS: 61-82-5 |
| Dicoumarol | Sigma-Aldrich | Cat# 2287897 CAS: 66-76-2 |
| Doxycycline | Sigma-Aldrich | Cat# D3072 CAS: 10592-13-9 |

| | | |
|---|---|---|
| IB-DNQ | Provided by Dr. Paul J. Hergenrother | N/A |
| β-Lapachone | MedChemExpress (MCE) | Cat# HY-13555<br>CAS: 4707-32-8 |
| LCS-1 | MedChemExpress (MCE) | Cat# HY-115445<br>CAS: 41931-13-9 |
| Z-DEVD-FMK (Caspase-3 Inhibitor) | Selleck Chemicals | Cat#: S7312<br>CAS: 210344-95-9 |
| Ferrostatin-1 | Selleck Chemicals | Cat# : S7243<br>CAS: 347174-05-4 |
| Matrigel® Basement Membrane Matrix | Corning Life Sciences | Cat# 354234 |
| Critical Commercial Assays | | |
| Aldefluor Assay kit | STEMCELL Technologies | Cat# 01700 |
| In Situ Cell Death Detection Kit (TUNEL assay) | Roche | Cat#11684795910 |
| Image-iT™ TMRM Kit | Invitrogen | Cat#I34361 |
| Mitochondria Isolation Kit | Sigma-Aldrich | Cat# 89874 |
| Extracellular Oxygen Consumption Assay kit | Abcam | ab197243 |
| Cellular Superoxide Detection Assay kit | Abcam | ab139477 |
| ATP Assay Kit | Beyotime Biotechnology | S0026 |
| MammoCult Human Medium Kit (for human tumorsphere culture) | STEMCELL Technologies | Cat# 05620 |
| Experimental Models: Cell Lines | | |
| Human: HCC1937 | ATCC | CRL-2336 |
| Human: HCC1806 | ATCC | CRL-2335 |
| Human: HCC70 | ATCC | CRL-2315 |
| Human: HCC38 | ATCC | CRL-2314 |
| Human: BT20 | ATCC | HTB-19 |
| Human: SUM149 and SUM159 | Stephen P. Ethier, Ph.D. | Medical University of South Carolina |
| MDA-MB-231 *NQO1*$^{+}$ and MDA-MB-231 *NQO1*$^{-}$ isogenic TNBC cell lines | Donated by the late Dr. David A. Boothman. | Indiana University School of Medicine, Indianapolis, IN 46202, USA |
| Vari068 TNBC cell line, derived from patient-derived xenograft tumors. | University of Michigan | N/A |
| Human: Hs578t | ATCC | HTB-126 |
| Human: MDA-MB-157 | ATCC | HTB-24 |
| Human: MDA-MB-231 | ATCC | CRM-HTB-26 |
| Human: MDA-MB-453 | ATCC | HTB-131 |

| | | |
|---|---|---|
| Human: MDA-MB-468 | ATCC | HTB-132 |
| Human: MCF7 | ATCC | HTB-22 |
| Human: ZR-75-1 | ATCC | CRL-1500 |
| Human: MCF10A | ATCC | CRL-10317 |
| Experimental Models: Organisms/Strains | | |
| Mouse strain: Fox Chase SCID | Charles River Laboratories | Strain Code: 236 |
| Recombinant DNA | | |
| TRIPZ Inducible Lentiviral Human NQO1 shRNA | Horizon Discovery | V2THS_235287 |
| TRIPZ Inducible Lentiviral Human SOD1 shRNA | Horizon Discovery | V3THS_369718 |
| TRIPZ Inducible Lentiviral Human SOD2 shRNA | Horizon Discovery | V3THS_307804 |
| TRIPZ Inducible Lentiviral Human CAT shRNA | Horizon Discovery | V2THS_150247 |
| SMARTvector Inducible Lentiviral Human NQO1 shRNA | Horizon Discovery | V3IHSHER_10771835 |
| SMARTvector Inducible Lentiviral Human NQO1 shRNA | Horizon Discovery | V3IHSHER_7177739 |
| SMARTvector Inducible Lentiviral Human NQO1 shRNA | Horizon Discovery | V3IHSHER_8909942 |
| SMARTvector Inducible Lentiviral Human SOD1 shRNA | Horizon Discovery | V3IHSHER_9961124 |
| SMARTvector Inducible Lentiviral Human SOD1 shRNA | Horizon Discovery | V3IHSHER_9099989 |
| TRIPZ Inducible Lentiviral shRNA Scrambled Control | University of Michigan vector core | N/A |
| Software and Algorithms | | |
| ELDA | WEHI Bioinformatics Resources | http://bioinf.wehi.edu.au/software/elda/index.html |
| FlowJo | FlowJo, LLC | https://www.flowjo.com/solutions/flowjo/ |
| GraphPad Prism | GraphPad Software Inc | http://www.graphpad.com/scientific-software/prism/ |
| ImageJ | NIH | https://imagej.nih.gov/ij/ |
| Compusyn | ComboSyn, Inc. | https://www.combosyn.com |